Chapter 7

ATMOSPHERIC TRANSPORT AND DEPOSITION OF γ–HCH TO THE ARCTIC REGION

This section contains a model evaluation of γ-HCH air concentrations, depositions and pathways of long-range transport to the Russian North in 1996 with the use of a source-receptor scheme. The realization of the source-receptor scheme used in this chapter is quite the same as for PCBs (see Chapter 6). γ-HCH emission sources were split into groups as described earlier in Chapter 4 (see also Fig. 7.19.a and b below).

γ-HCH transport was simulated for the period from 1990 to 1996 to evaluate accumulation in main environmental media (soil, seawater, vegetation).

The calculations are made by using the hemispheric version of the MSCE-POP model (see Section 3.3 above) and cover the territory of the whole Northern Hemisphere. Such spatial coverage is reasonable for the assessment of γ–HCH contamination of the Russian North from remote regions such as North America and Asia.

7.1. General description of modeling results

Redistribution between environmental media

In the course of the model run for the period from 1990 to 1996, detailed spatial distributions of contamination in main environmental media (atmosphere, soil, seawater and vegetation) as well as deposition fluxes over the Northern Hemisphere with resolution 2.5°×2.5° were obtained under the assumption that initial media content in the beginning of 1990 is zero. These results were used to assess the contents of main media over the whole hemisphere (that is, the total amount of the pollutant accumulated in such media as atmosphere, soil, seawater and vegetation) in 1996 and to examine the dynamics of the accumulation process. Figure 7.1 displays trends of γ–HCH accumulations during the simulated period (1990–96) in these media. For the sake of comparison, the dynamics of γ–HCH emissions used in modeling is also presented.

According to the emission data used, total emissions in the Northern Hemisphere decreases from 1990 to 1991, and then remains at an approximately constant level (Fig. 7.1.a). It can be observed that the process of accumulation takes place differently in each environmental compartment. Namely, the dynamics of γ–HCH content in the atmosphere and vegetation follows the emission dynamics (Figs. 7.1.b and c). Contents in soil and seawater (Figs. 7.1.d and e) grow quickly during the first three years of the simulation period and beginning in 1993 become more or less stable.

Since a stabilization of content in all the environmental media has been reached to some extent by the end of 1996, redistribution of γ–HCH in the end of the simulation period allows one to select media with the highest accumulation of the pollutant. The redistribution of γ–HCH between environmental compartments over the whole Northern Hemisphere by the end of the simulation period is shown in Figure 7.2.

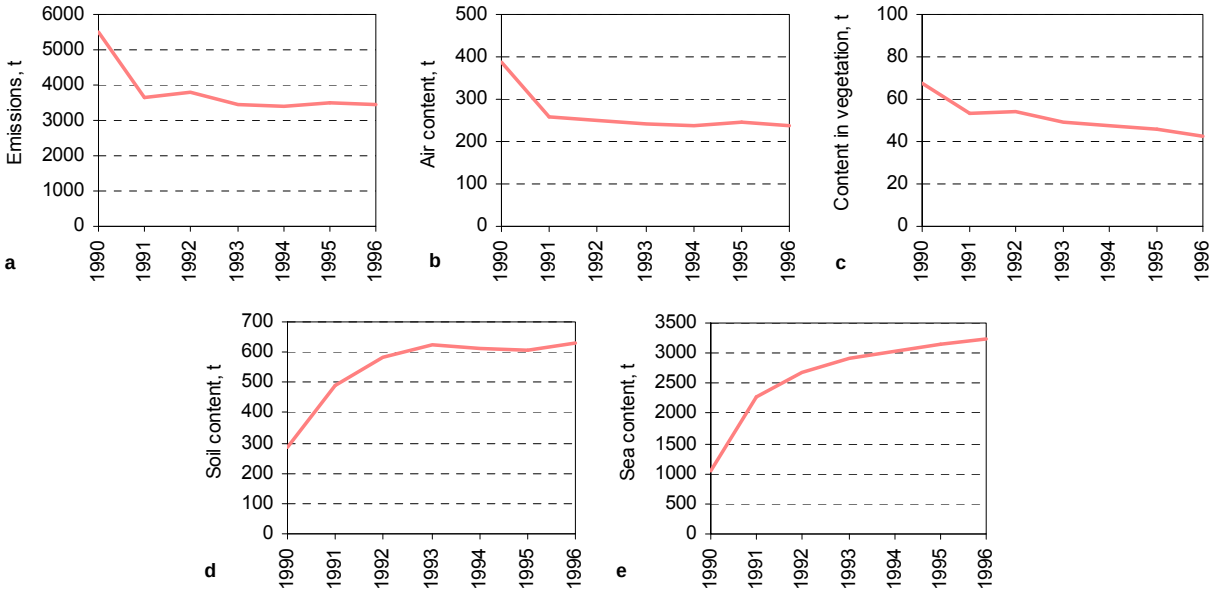

Figure 7.1. *Trends of γ–HCH emissions and accumulation in main environmental media and in the whole environment during 1990 – 1996 (calculations with initial media content equal to zero)*

According to this distribution seawater is the main media accumulating γ–HCH (it contains about 80% of the whole environmental content). This conclusion coincides with that made in [*Strand and Hov*, 1996]. Thus, atmosphere/gas exchange, transport by sea currents and the influence of sea ice (see Annex E) seem to be essential in the description of the fate γ–HCH in the environment. Soil accumulated a somewhat less, though still considerable fraction of γ–HCH.

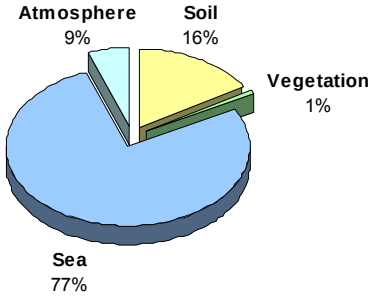

Figure 7.2. *Calculated redistribution of γ-HCH between environmental compartments by the end of 1996*

Spatial distribution of contamination

Further, calculation results allow one to perform more detailed analysis of the contamination of environmental media, that is, to evaluate spatial distribution of γ–HCH contamination by the end of the simulation period (1996). Figure 7.3 shows spatial distributions of average annual γ–HCH depositions and concentrations in the lower atmospheric layer and upper seawater layer in comparison with that of emissions.

Maps of concentrations and depositions indicate that high levels of concentrations and depositions are mainly characteristic of regions with high emissions. However, the transport of γ–HCH from emission sources to remote regions both in the atmosphere and sea is also noticeable (e.g. atmospheric transport from European and Indian sources towards the North-East). This will be demonstrated below in more detail

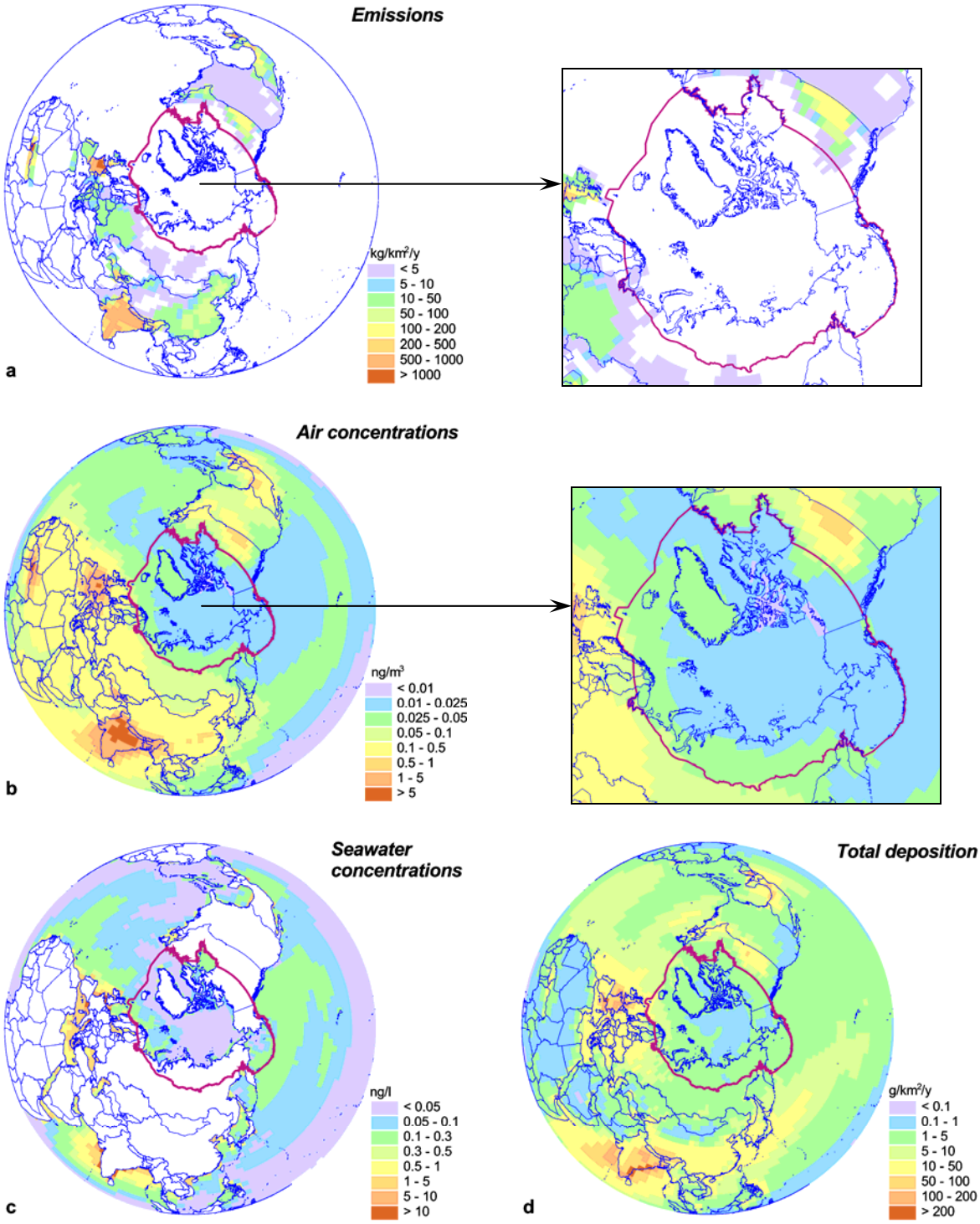

Figure 7.3. *Calculated spatial distribution of average annual γ–HCH deposition and concentrations in atmosphere and seawater in comparison with emissions for 1996*

Contamination of the Arctic region

Calculated spatial distributions of air concentrations and depositions allow us to evaluate pollution levels in the Arctic (AMAP region, see Fig. 7.3). Table 7.1 contains the annual averages of air concentrations and depositions over the Arctic calculated for 1996.

Table 7.1. *Annual averages of air concentrations and deposition flux in the Arctic region in 1996*

	Min	Max	Aver
Air concentrations, ng/m^3	0.0086	0.11	0.023
Deposition flux, g/km^2/y	0.22	17	2.4

The calculated total amount of γ-HCH deposited to the Arctic region in 1996 equals 78 tonnes. Due to the high deposition velocity over sea (according to the model assumption it is twice higher on the average than that over land) and taking into account that an essential part of the area is covered by ocean (about 60% according to [*AMAP,* 1998]) the total amount of γ-HCH deposited to sea area in 1996 is estimated at 58 tonnes. Due to the high persistence of the pollutant in a sea environment, depositions of γ-HCH to seawater for the period from 1990 to 1996 form sufficiently high seawater concentrations in the region (up to 1 ng/l and more). It must be taken into account that at present the model underestimates seawater concentrations since some pathways of the pollutant to the region are not taken into account (e.g., inflow with rivers).

Modeling results allow one also to evaluate the contributions of different emission sources to the contamination of the Arctic region (Fig. 7.4). The main group of sources contributing this region is Western Europe (about 40%), followed by India (19%), America (17%), China (10%) and Russia (6%). The share of all other sources amounts to 8%.

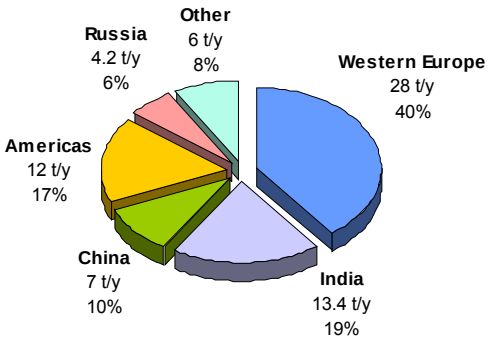

Figure 7.4. *Contributions of different emission sources to the deposition to the Arctic region in 1996*

In spite of the fact that anthropogenic emissions in the Arctic region are practically nonexistent (Fig. 7.3.a) contamination in this region is noticeable. Here air concentration levels can reach up to 0.11 ng/m^3, and deposition flux can reach 17 g/km^2/y. Seawater concentrations near the regions of the Russian North are in the range 0.1 – 2 ng/l. These concentrations (as well as concentrations in soil) are the result of long-term accumulation process (see above) and the so-called cold condensation effect. To demonstrate this effect latitudinal distributions of contamination in main media in the polar region (60º and higher) were calculated (since there is no soil at latitudes higher than 80º, the plot for soil concentrations is presented for latitudes from 60º to 80º only).

Calculations show that though main emission sources are located in the middle latitudes (not higher than 70 degrees North), concentration levels in all main environmental compartments show a very slow decrease in the polar zone concurrent with latitude (or no decrease at all, see Figs. 7.5.a–c). This effect can be explained by more effective accumulation of γ–HCH at low temperatures and indicates that this pollutant tends to accumulate in regions with a cold climate.

One more proof of ***cold condensation*** is demonstrated by the comparison of the latitudinal distribution of soil concentrations with that of emissions (Fig. 7.6).

From the plot it is seen that maxima in latitudinal distribution of soil concentrations shift to the north with respect to maxima of emission distribution and the maximum of soil concentrations located at higher latitudes is much more pronounced.

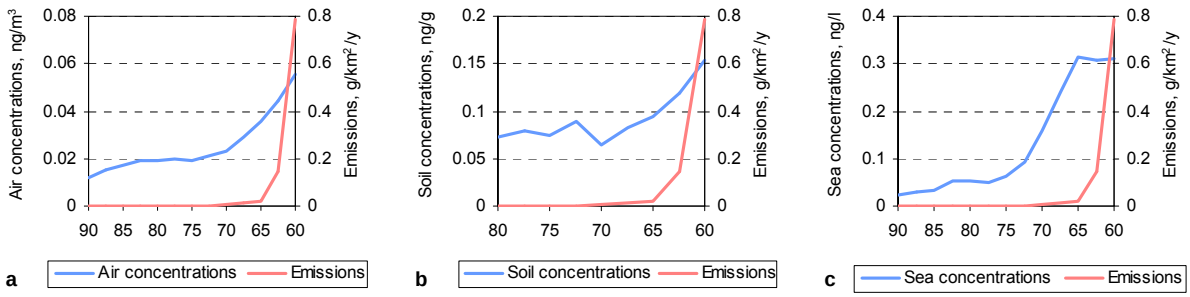

Figure 7.5. *Calculated latitudinal distribution of γ–HCH concentrations in the atmosphere (a), soil (b) and seawater (c) in the polar zone*

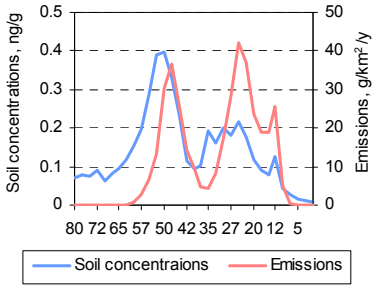

Figure 7.6. *Calculated latitudinal distribution of γ-HCH concentrations in soil over the whole hemisphere*

Pathways of atmospheric γ-HCH transport to the Arctic

Spatial distributions of contamination calculated over the entire Northern Hemisphere allow one also to evaluate pathways of γ–HCH transport from different groups of sources to the Arctic in various media.

Here we present the analysis of γ–HCH transport from the two largest groups of sources: India and West Europe. The process of atmospheric transport of γ–HCH from Indian sources in 1996 under the assumption of initial concentrations of zero in all environmental compartments is displayed month by month in Figure 7.7.

One can see that in the beginning of the year (January – March) γ–HCH transport takes place mainly in an eastward direction. From April to August γ–HCH is transported in a northward direction to the Russian North and the Arctic region due to the cyclonic character of wind patterns in the region. Then the character of wind patterns change and from September the process of atmospheric outflow from the Arctic and transport in an eastward direction takes place. In accordance with model estimates, γ–HCH from Indian sources can be transported to the Russian North and the Arctic region passing around Tibet from its southern-eastern side.

The transport from West-European sources is shown in Figure 7.8.

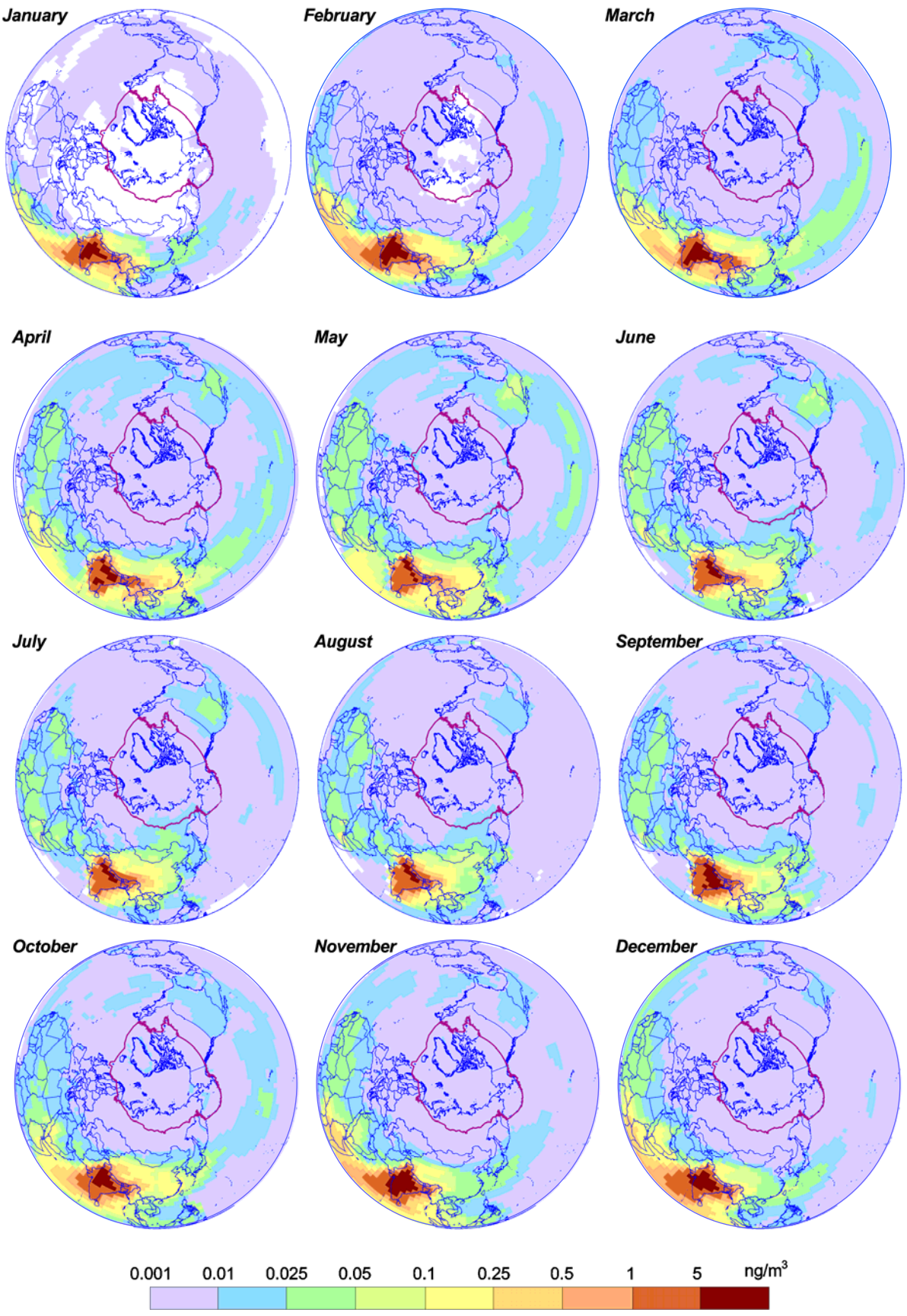

Figure 7.7. *Monthly dynamics of γ–HCH transport from Indian sources for 1996 (air concentrations)*

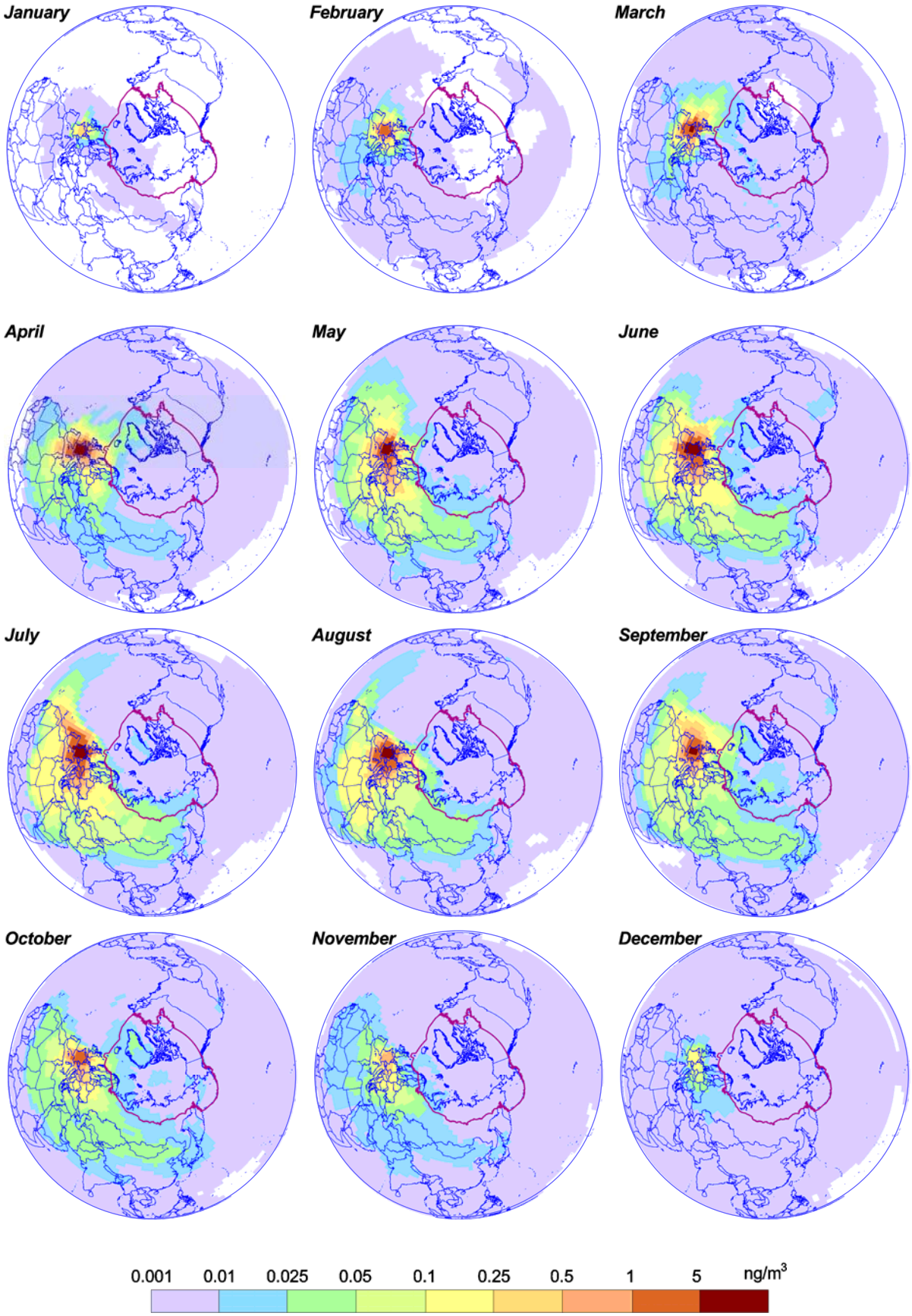

Figure 7.8. *Monthly dynamics of γ–HCH transport from West-European sources for 1996 (air concentrations)*

Maps of monthly averaged air concentrations show that the transport of γ–HCH from West-European sources to the Arctic as a whole and to the Russian North in particular takes place from January to September in eastward and north-eastward directions. The decrease of air concentrations in the period from October to December is explained by an emission decrease due to seasonal variations assumed in the model for this group of sources (see Section 4.3).

This analysis can be extended to the analysis of source-receptor relationships for selected regions of the Russian North. This will be done below (see Section 7.4).

Calculated spatial distributions of γ–HCH contamination in the Northern Hemisphere also make it possible to calculate average contamination levels in region-receptors. However, prior to that we wish to present a description of comparison between measurements and calculations to elucidate the reliability of calculated estimates.

7.2. Comparison of modeling results with measurements

The aim of this section is to compare calculated values of air concentrations and depositions with available measurement data. For the comparison we used annual averages of measured γ–HCH concentrations in the ambient air and precipitation for the period from 1990 to 1996, available in the EMEP database (Chemical Coordinating Centre of EMEP) [*Lövblad et al.*, 1995, *Berg et al.*, 1996, *Berg et al*., 1997, *Berg and Hjellbrekke*, 1998, *Berg and Hjellbrekke*, 1999]. Part of the air concentration values calculated for the Arctic region were compared with measurement data available in [*AMAP,* 1999]. In addition, results of national measurement campaigns [*Brorström-Lundén et al.,* 2000; *Reviews of the environmental background ….*, 1994 – 1996, *Hoff et al.,* 1996, IADN Results to 1996] and some literature data [*Halsall et al*., 1998; *Harner et al.,* 1999] were included in the comparison study carried out for air concentrations of different regions of the Northern Hemisphere. However, taking into account that computation period begins from 1990, sufficient accumulation levels in media are achieved only by 1993 and we carry out the comparison for the period from 1993 to 1996.

Figure 7.9 presents a map of the geographical locations of measurements used for the comparison. The map indicates that measurement data are available for different regions: North-west Europe, the Arctic zone, the Great Lakes region, and the Baikal region. It is readily seen that the monitoring data on γ-HCH concentrations in air, in contrast to those in precipitation, were available for a number of measurement sites situated in the Arctic region specifically (Pallas, Ny Ålesund, Tagish, Dunai, Alert, etc.). As evident from the map, spatial coverage of air concentration measurements is much larger than that of precipitation. The majority of sites monitoring γ–HCH concentration in precipitation are located in Europe. Certainly, for better validation of calculation results more measurements both in air and in precipitation are needed.

Figure 7.9. *Location of measurement sites used for the comparison. Circles: measurements of air concentrations, triangles: measurements of concentrations in precipitation*

In the comparison, annual means of γ-HCH measurements in air and precipitation were used. Namely, mean annual air concentrations are mean arithmetic values of presented data. Mean concentration in precipitation is precipitation weighted arithmetic average. All the measured values were statistically processed. Additionally, all data have been checked for outliers. For example, very high values in the EMEP database, which are beyond the scope of four-fold mean root square deviation in the log–normal distribution have not been taken into account. It might well be pointed out that available observed data, as a rule, cover prolonged time periods thereby providing the possibility to compare the dynamics of air and precipitation contamination by γ-HCH for a given monitoring station.

7.2.1. Air concentrations

Table 7.2 contains the comparison results of measured and calculated concentrations in the surface air layer of the European and Arctic regions for the period from 1993 to 1996.

Table 7.2. *Comparison of measured and calculated values of concentrations in the surface air layer, pg/m^3 and calculation to measurement ratio for Europe and the Arctic*

Site	Location		Year	Measured			Calculated	Calc/meas ratio
	Long	Lat		Min	Max	Aver		
SE2 [1)]	11.93	57.42	1994	11	199	51.2	195.00	3.81
			1995	6	78	25	176.00	7.04
			1996	6	50	26	167.00	6.42
SE12 [5)]			1996			83.43	74.6	0.89
NO99 [2)]	6.56	58.1	1993	12.1	282.7	53.52	178.00	3.33
			1994	1.99	1000.3	122.89	160.00	1.30
			1995	7.4	593.5	64.98	149.00	2.29
			1996	15.8	132.6	60.72	154.00	2.54
NO42 [3)]	11.88	78.9	1993	3.3	38.3	14.4	25.00	1.74
			1994	5.31	62.1	16.1	24.00	1.49
			1995	5.98	41.1	13.13	23.20	1.77
			1996	4.87	39.1	12.85	20.00	1.56
FI96 [1)]	24.12	67.97	1996	4.2	24	11	54.2	4.93
IS91 [4)]	-20.25	63.45	1995	0	50	14.19	36.8	2.59
			1996	3.6	32.3	9.64	33.6	3.49
Tagish [5)]	-134.27	60.3	1993	3.33	25.1	10.95	15.9	1.45
			1994	4.36	138	14.21	15.8	1.11
Alert [5)]	-62.5	82.45	1993	1.92	410	18.53	15	0.81
			1994	0.15	57.85	10.7	14.6	1.36
Barguzin BR [6)]	109.5	54.2	1993	2.0	204	15	104	6.93
			1994	2.0	366	38	92.8	2.44
			1995	3.0	860	154	87.1	0.57
Dunai [7)]	124.5	74.99	1993	3.68	22.7	9.83	27.4	2.79
Barents Sea [8)]	43.7	76.4	1996	13.3	67.8	36.2	16.7	0.46
North East Arctic [8)]	-85.2	83.7	1996	5.3	35.6	14.9	20.5	1.38
North Pole [8)]	-166.1	88.3	1996	12.2	18.8	15	14.9	0.99
Average								2.5
Correlation between measured and calculated values								0.5

[1)] *Brorström-Lundén et al.*, 2000
[2)] *Berg et al*., 1996; *Berg and Hjellbrekke*, 1998
[3)] *Berg et al*., 1996; *AMAP*, 1999
[4)] *Berg et al*., 1996; *Berg et al*., 1997
[5)] *AMAP*, 1999
[6)] *Reviews of the environmental background ….* 1994 – 1996
[7)] *Halsall et al*., 1998
[8)] *Harner et al*., 1999

The ratios of calculated to measured values (see last column of Table 7.2) show that ***the model on average overestimates air concentrations 2.5 times and the correlation between calculated and measured values is 0.5***. A good agreement is obtained at the Canadian sites Alert and Tagish (located inside the Arctic region); measurement data were taken from [*AMAP*, 1999]. Large discrepancies are obtained at Swedish site SE2 (Rörvik) [*Brorström-Lundén et al.*, 2000]. However, at Swedish site SE12 (Aspvreten), calculations and measurements [*AMAP*, 1999] agree well enough. Most likely reason for these discrepancies in connected with uncertainties in spatial distribution of emissions.

Large discrepancies between measurement and modeling results occur at the Great Lakes sites [*Hoff et al.*, 1996, *IADN Results to* 1996]. However, because spatial distribution of emissions from Canada is of a conventional character (it is based on crop area distribution and as a result a large amount of emissions in Canada is assumed to be located near the Great Lakes region) these measurements were not included into the comparison. Refinement of spatial distribution of emissions in this region should improve agreement between calculated and measured concentrations in this region.

The results of the comparison are presented in the form of a scatter plot. The scatter plot in the Figure 7.10 illustrates differences between calculated and measured annual air concentrations. Most of computed concentrations are within a factor of five with respect to measured values. The zone of "factor of fife" is shown in the diagram by the dashed lines. When the station is located within this zone, annual average computed value for this station is no more than five times higher or no less than five times lower than the measured value. A logarithmic scale is applied for better display of the entire range of measured and computed values. The measurements at the Great Lakes are depicted by blue triangles. Over 75% of comparisons are within a factor of four.

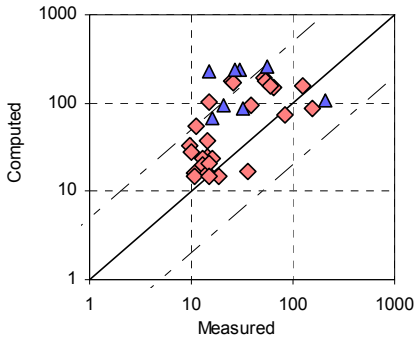

Figure 7.10. *Computed versus measured annual average γ-HCH concentrations in air in 1996, ng/m^3*

From the plot it is seen that only three values are outside factor five (except for measurements near the Great Lakes).

7.2.2. Concentrations in precipitation

Table 7.3 presents the comparison between calculated and measured mean annual concentrations in precipitation. Available measurement data on γ-HCH content in precipitation were obtained at the EMEP monitoring stations. As it was mentioned above, these data cover only the European region, in particular its northern part.

For the concentration in precipitation, all computed values are within a factor of three with respect to measurements, with an average measurement to calculation ratio of 1.15. The correlation between measured and computed values is 0.82. It should be mentioned that a satisfactory correlation of γ-HCH concentrations in air and precipitation is due to more reliable emission distribution in the European region taken from [*Pacyna et al.*, 1999] and used in our model calculations.

Table 7.3. *Comparison of measured and calculated values of concentrations in precipitation, ng/l and calculation to measurement ratio*

Site	Location		Year	Measured			Calculated	Calc/meas ratio
	Long	Lat		Min	Max	Aver		
DE1 [1)]	8.3	54.9	1993	3.2	80.5	9.28	7.60	0.82
			1995	0.13	20.0	6.32	7.02	1.11
			1996	1.8	180	10.38	7.09	0.68
DE9 [2)]	12.7	54.4	1995	0.13	20.0	6.52	5.57	0.85
IE2 [2)]	6.4	53	1994	0.05	5.2	1.43	2.65	1.85
			1995	0.5	7.5	2.15	2.63	1.22
			1996	0.5	8	2.04	2.74	1.34
IS91 [3)]	20.3	63.6	1995	0	6.83	0.44	0.89	2.02
			1996	0.07	2.6	0.27	0.76	2.81
NO99 [2)]	6.5	58.1	1993	0.83	74.36	8.45	4.34	0.51
			1994	0.61	70.6	9.98	4.06	0.41
			1995	0.66	60.46	5.54	3.88	0.70
			1996	2.06	24.6	8.01	4.47	0.56
Average								1.15
Correlation								0.82

[1)] *Lövblad et al.*, 1995 [2)] *Berg et al.*, 1996 [3)] *Berg and Hjellbrekke*, 1999

The scatter plot in Figure 7.11 illustrates differences between calculated and measured annual concentrations in precipitation. The 'factor of two' agreement between computed and measured annual concentrations lies between the dashed lines. As in the case of air concentrations, logarithmic scale is applied.

It is seen that ***about 80% of all computed concentrations are within a factor of two with respect to measured values***.

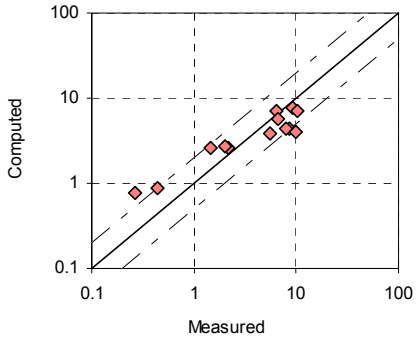

Figure 7.11. *Computed versus measured annual average γ-HCH concentrations in precipitations in 1996, ng/l*

7.3. Concentration and deposition levels in regions-receptors

This section is devoted to evaluation of concentration levels and their seasonal variations in five regions-receptors:

- Murmansk Oblast (MUR),
- Nenets Autonomous Okrug (NEN),
- Yamalo-Nenets Autonomous Okrug and Taimyr Autonomous Okrug (YNT),
- Sakha Republic (Yakutia, YAK),
- Chukotka Autonomous Okrug (CHU).

Spatial distributions

Figures 7.12–7.14 illustrate levels of air concentrations and depositions in five regions-receptors in the Russian North obtained by the end of calculation period (1996). Because of importance of marine environment for γ–HCH we present also the map of seawater concentrations.

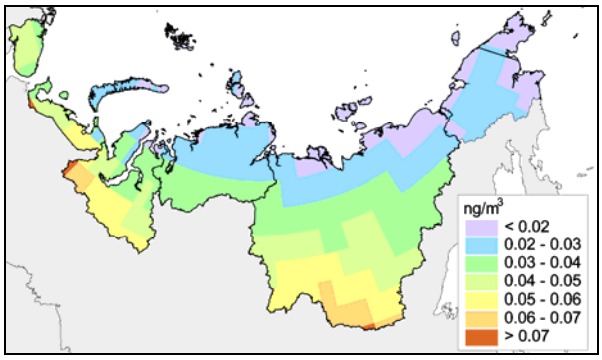

Figure 7.12. *Air concentrations in the Russian North calculated for 1996*

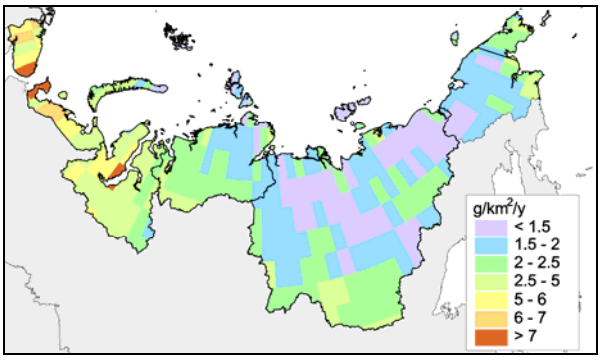

Figure 7.13. *Deposition in the Russian North calculated for 1996*

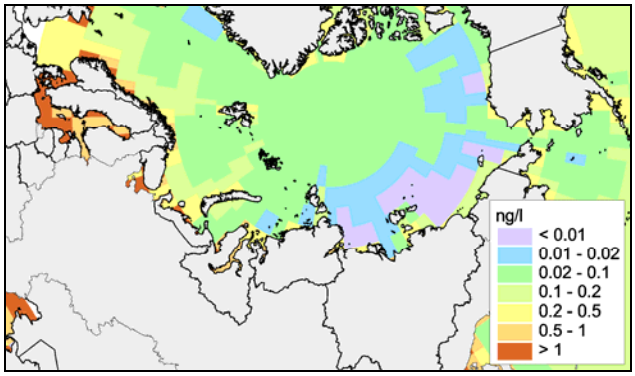

Figure 7.14. *Seawater concentrations near the Russian North calculated for 1996*

Higher air concentration levels (from 0.02 to 0.07 ng/m^3) are characteristic of Murmansk Oblast, Nenets AO and of the south of Yamalo-Nenets AO and Sakha Republic. Lower levels (from 0.01 to 0.3 ng/m^3) are characteristic of Taimyr AO, Chukotka AO and of the north of Sakha Republic. Similarly, deposition fluxes are larger for Murmansk Oblast, Nenets AO and Yamalo-Nenets AO (from 2 to 7 g/km^2/y and more) and lower in Taimyr AO, Sakha Republic and Chukotka AO (0.1 – 3 g/km^2/y).

Calculated marine concentrations near borders of the Russian North regions are from 0.01 to 1 ng/l. The map of marine concentrations illustrate also that the inflow of γ–HCH from European sources with sea currents take place mainly from the North Atlantic: higher concentrations are calculated near the Northern part of the Scandinavian Peninsula and Spitsbergen. This fact agrees with evaluation of marine inflow of γ-HCH to the Arctic made in [*AMAP*, 1998]. We note, however, that at present the model underestimates concentrations in seawater. At present development of model descriptions of seawater and soil environments is in progress (see Annexes D, E).

Annual averages and their spatial variations

On the basis on the above spatial distributions (Figs. 7.12–7.14) average levels of deposition and air concentration levels in regions-receptors and their spatial variations were evaluated. The results are shown in Figure 7.15 (bars mean spatial variations of annual means inside each region). The corresponding numerical values are presented in Table 7.4.

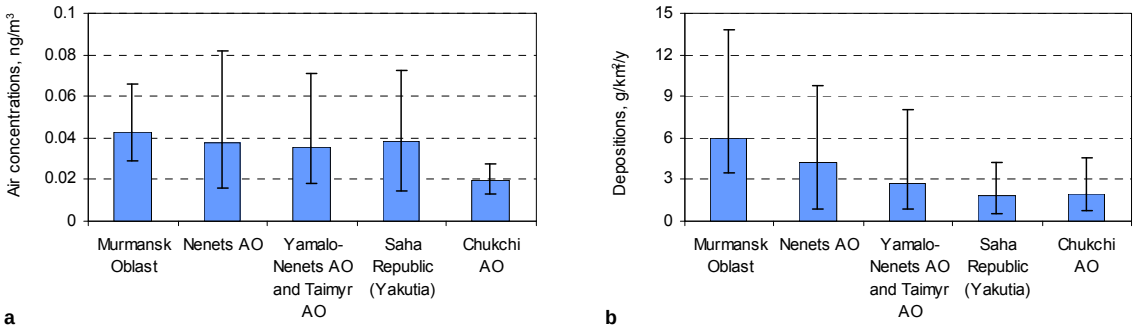

Figure 7.15. *Contamination levels in the regions of the Russian North calculated for 1996: annual averages and their spatial variations: air concentrations (a), depositions (b)*

Table 7.4. *Deposition and air concentration levels in regions-receptors*

Region	Air concentrations, ng/m^3			Deposition flux, g/km^2/y		
	Min	Max	Aver	Min	Max	Aver
Murmansk Oblast	0.029	0.066	0.043	3.5	13.8	6.0
Nenets AO	0.016	0.082	0.038	0.9	9.7	4.3
Yamalo-Nenets AO and Taimyr AO	0.018	0.071	0.036	0.8	8.0	2.7
Sakha Republic	0.014	0.072	0.038	0.5	4.3	1.8
Chukotka AO	0.013	0.027	0.020	0.75	4.6	1.9

The calculated air concentration levels in the first four regions (Murmansk Oblast, Nenets AO, Yamalo-Nenets AO and Taimyr AO, and Sakha Republic) are similar. Average concentrations in Chukotka AO are two times lower. This is explained by the geographical location of the latter region. Annual averages of deposition flux values change more essentially from region to region. This is mainly caused by different values of precipitation flux in these regions (see below the analysis of seasonal variations).

Up to the moment we have considered annual averages of concentrations and depositions. However, seasonal variations of air concentrations and depositions are high in the northern regions due to high temperature changes and play an important role for the Arctic region. Below we consider seasonal variations of air concentrations and depositions for all five regions-receptors.

Seasonal variations

Monthly averages of air concentrations and depositions for Murmansk Oblast are presented in Figure 7.16 together with variations of temperature and precipitation amount.

Monthly averages of atmospheric concentrations in Murmansk Oblast vary from 0.02 to 0.07 ng/m^3. It is seen that maximum concentrations are reached in August and September. This is due to high

enough temperatures (5 – 10º C) and by seasonal variations of emissions. Dry deposition flux (flux of gaseous exchange) is determined by atmospheric concentrations and temperature. The dependence of this flux on temperature is inverse. Namely, the more temperature is, the less are atmosphere/soil and atmosphere/sea exchange fluxes. For instance, moderate values of air concentrations and high enough temperature in June (10º C) lead to the decrease of dry deposition flux compared with values in neighbouring months. In addition wet depositions are affected by precipitation amount. In particular, this is the reason for higher value of wet deposition flux in July in comparison with that in June and August.

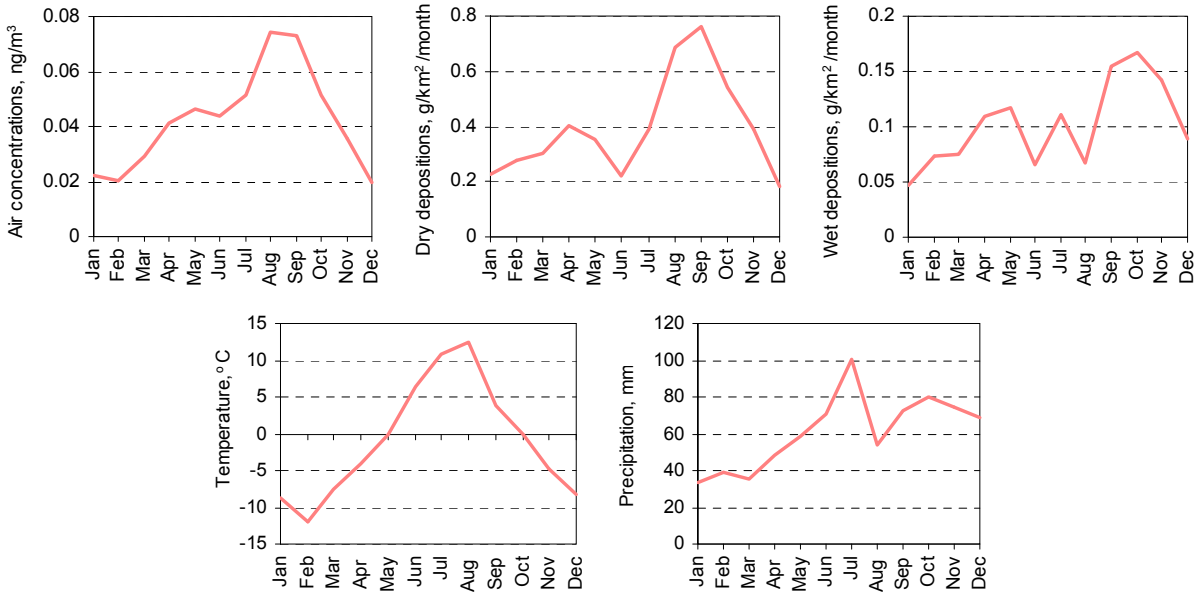

Figure 7.16. *Seasonal variations of air concentrations and depositions (in comparison with temperature and precipitation amount) in Murmansk Oblast*

Plots of seasonal variations for the rest four regions of the Russian North are presented in Figure 7.17. For comparison Figure 7.18 displays plots of monthly averages of temperature and precipitation in these four regions.

The processes determining concentrations and depositions in these regions are of the same character as above. Less concentration levels in Chukotka AO are explained by their larger distance from main emission sources. Comparatively high values of wet deposition flux in this region with lower air concentrations are explained by high values of precipitation amount which are about 1.5 times higher than in Nenets AO, Yamalo-Nenets AO and Taimyr AO, and Sakha Republic. It is seen that minimum values of wet deposition flux correspond in general to minima of precipitation amount for each region. Close to constant values of dry deposition flux from January to April in Sakha Republic and Chukotka AO is explained by relatively low rate of increase of atmospheric concentrations together with high temperature gradients which are characteristic of these regions.

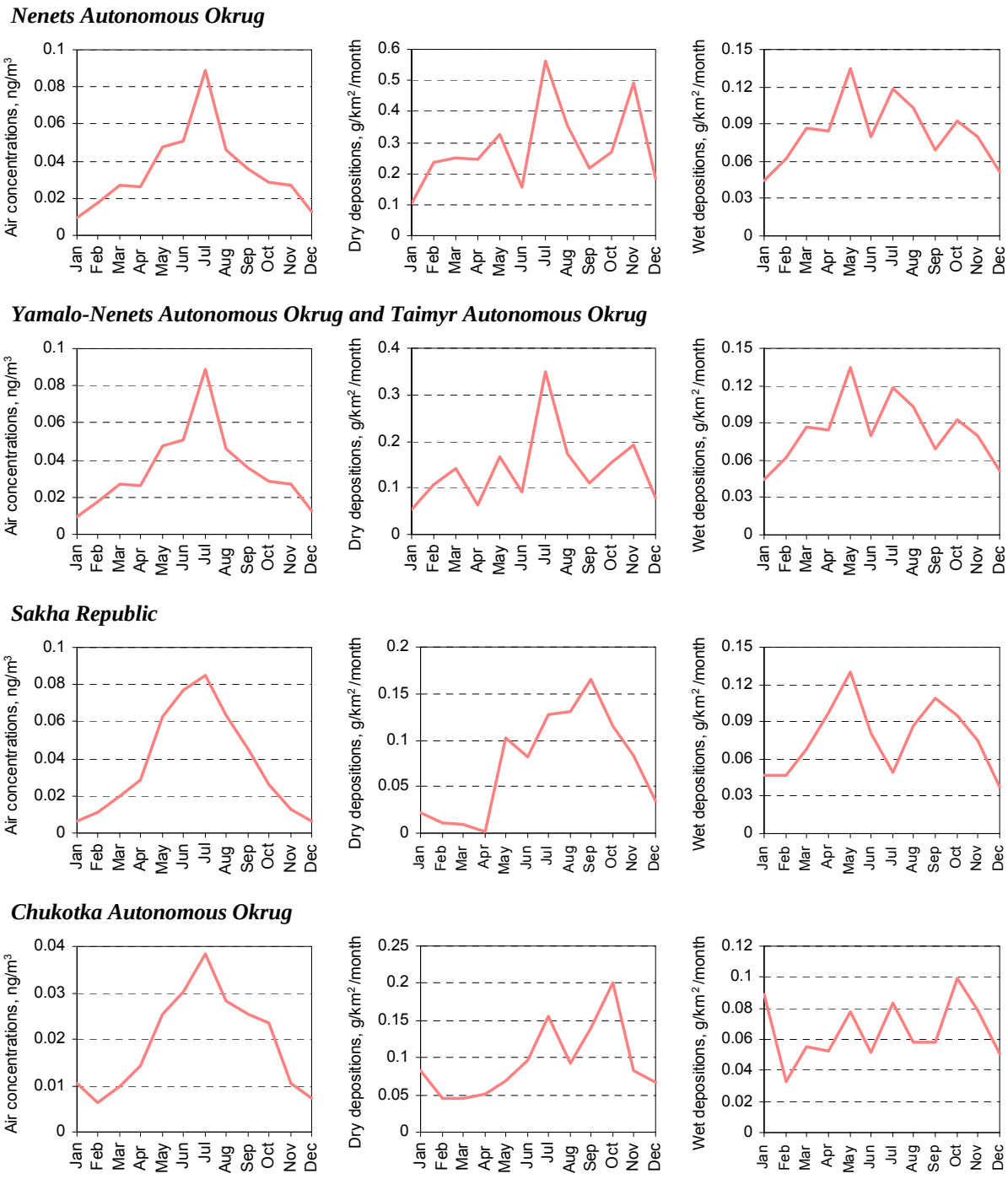

Figure 7.17. *Seasonal variations of air concentrations and depositions in four regions of the Russian North*

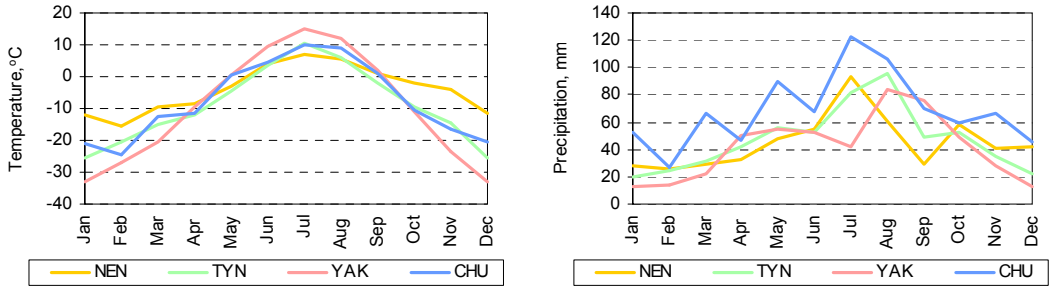

Figure 7.18. *Seasonal variations of temperature and precipitation amount in four regions of the Russian North*

7.4. Source-receptor relationships

Contamination in regions-receptors is formed both by emissions of the considered year (1996) and by amount of pollutant accumulated in the environment during the period preceding the reference year (1990 – 1995). Calculations show that about 40% of concentrations in soil and seawater over regions of the Russian North are formed by γ-HCH earlier accumulated in environmental media.

Similar to the case of PCBs keeping in mind that the historical emission cannot be controlled by any political decisions we shall pay the main attention to deposition from anthropogenic sources. Namely, the influence of different groups of sources on the contamination of regions-receptors is evaluated. The analysis of contributions from different sources is preformed into two steps. First we use rough splitting of sources within the Northern Hemisphere. Namely, we combine all Russian sources in one group (Fig. 7.19.a). Then we use more detailed splitting of Russian sources (Fig. 7.19.b).

Names of Russian source groups influencing the contamination of the Russian North together with their abbreviations are presented in Table 7.5.

The contributions of different groups of sources to the total hemispheric emissions are shown in Figure 7.20.

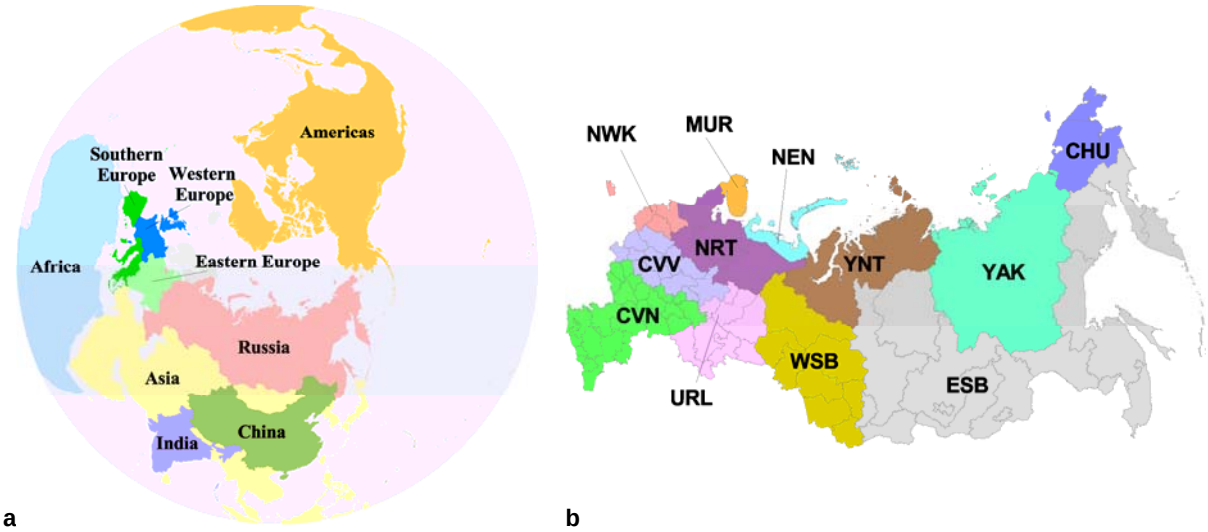

Figure 7.19. *Splitting emission sources into groups, (a) – rough scheme, (b) – specification of Russian sources*

Table 7.5. *γ-HCH source groups in the Russian Federation*

Name	Abbreviation	Name	Abbreviation
Murmansk Oblast *	MUR	North-Western region and Kaliningrad Oblast	NWK
Nenets AO	NEN	Central and Volga-Viatsky regions	CVV
Yamalo-Nenets AO and Taimyr AO	YNT	Central-Chernozem, Volga, and North-Caucasian regions	CVN
Sakha Republic (Yakutiya)	YAK	Ural region	URL
Chukotka AO	CHU	West-Siberian region	WSB
Northern region	NRT	East-Siberian and Far-Eastern regions	ESB

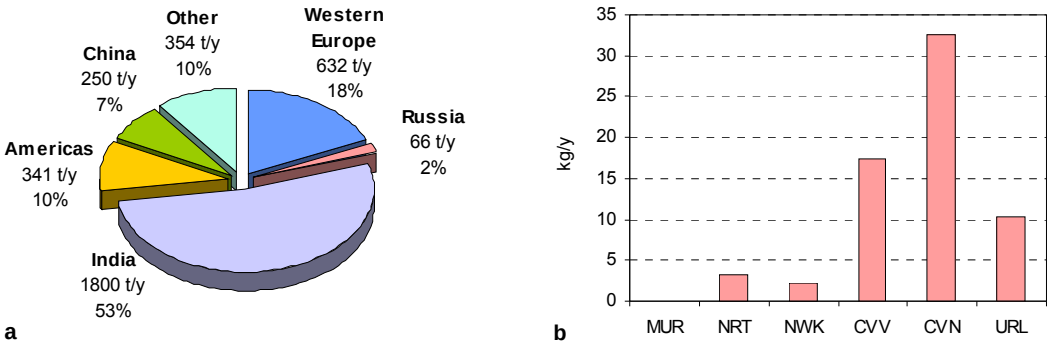

Figure 7.20. *Contributions of different emission source groups to the hemispheric emissions in 1996: rough scheme (a), detailed splitting of Russian sources (b)*

Due to local peculiarities and peculiarities of the wind pattern the contributions of these groups to the contamination of regions-receptors can be different from that shown in Figure 7.20 for emissions.

Murmansk Oblast. We begin with the consideration of contributions of these source groups to depositions and concentrations in main environmental media (atmosphere, soil, seawater) first with rough splitting scheme where all Russian sources are considered as one group.

Sources of West-Europe make the largest contribution to deposition to Murmansk Oblast (more than 50%). Russia is responsible for 17%. Then come India (9%), North America (7%) and China (4%). Contributions of all other sources account for 9% (Fig. 7.21).

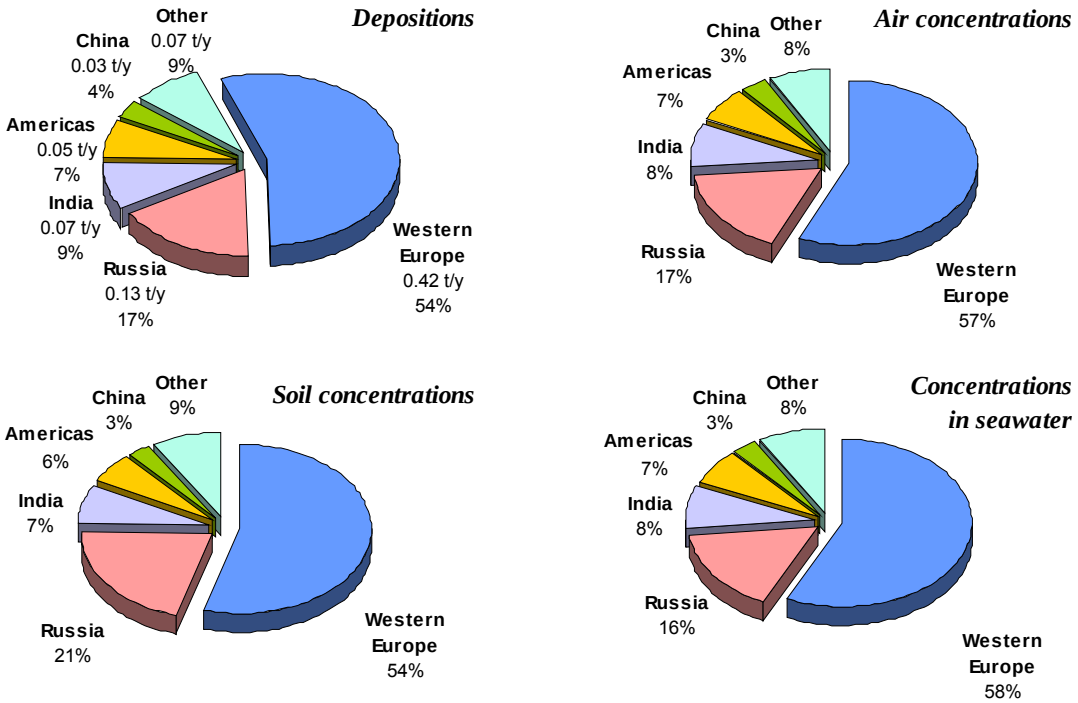

Figure 7.21. *Contributions of different emission source groups (rough scheme) to annual mean air concentrations and depositions for Murmansk Oblast in 1996*

It is seen that contributions of different source groups to all media are almost the same as for depositions. Similar situation is observed also for other regions-receptors. Below we shall present pie charts for depositions only.

The detailed analysis of Russian contribution to Murmansk Oblast is presented in Figure 7.22.

Russian contribution to depositions to Murmansk Oblast is mostly made by Central and Volga-Viatsky regions (40 kg or 5.1%) and Central-Chernozem, Volga, and North-Caucasian regions (34 kg or 4.3%). Then comes the contribution from the Northern region (23 kg or 2.9%) and from Murmansk Oblast itself (19 kg or 2.4%). The inputs from the north-western region and Kaliningrad Oblast and Ural region are comparatively small.

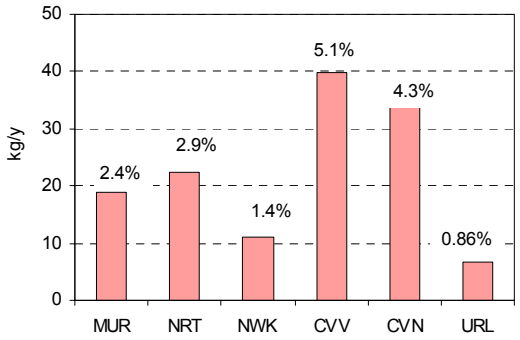

Figure 7.22. *Relative inputs of different groups of Russian emission sources to the overall Russian contributions to depositions to Murmansk oblast*

The inputs of different emission sources to deposition to the considered region are subject to seasonal variations determined both by seasonal variations of emissions and by differences in meteorological conditions. Figure 7.23 displays seasonal variations of contributions of main source groups to deposition to this region in absolute (a) and relative (b) values in 1996.

As it was shown above, main contributions to depositions to the region are made by Western Europe and Russia. Due to seasonal variations of emissions from both source groups their contributions to deposition to the region enlarge from the first to second quarter. However, due to wind pattern (on the average winds of western direction are prevailing in the region) the contributions from Western Europe are growing faster than that from Russian sources. This leads to a slight growth of contribution to depositions from Western Europe sources and diminishing of contribution of Russian sources. This process is even more pronounced from second to third quarters since in this period northern and western wind directions are prevailing in the region. In the fourth quarter due to emission reduction the contribution from Russian sources drops and it becomes comparable with contributions from American, Chinese and Indian sources. This leads to further decrease of relative contributions from Russian sources to overall deposition to the considered region.

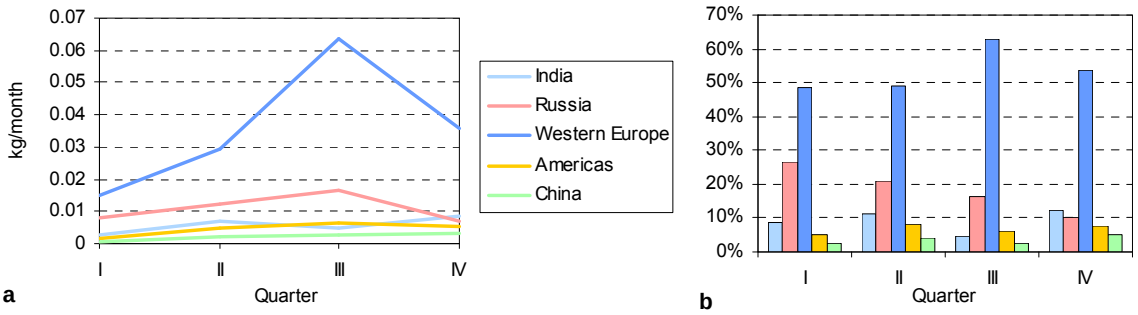

Figure 7.23. *Seasonal variations of contributions of different groups of emission sources to depositions to Murmansk Oblast in 1996*

Nenets Autonomous Okrug. For this region the order of main contributors to depositions is the same as for Murmansk Oblast. However, the contribution of West Europe is decreased and of Russia is increased. This is evidently caused by geographical location of source groups with respect to receptors. The structure of Russian contribution to depositions to this region is similar to that for Murmansk Oblast though the influence of Ural region increases. The main exception is that the contribution of sources of Murmansk Oblast to depositions is negligible for this region.

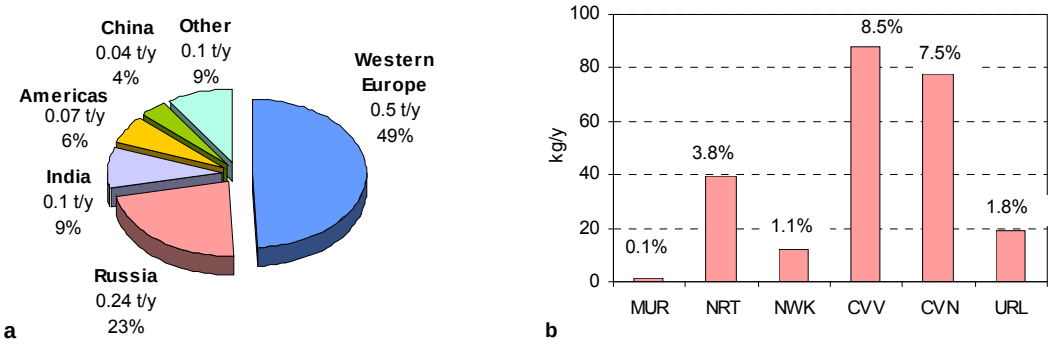

Figure 7.24. *Contributions of different emission source groups to annual depositions for Nenets AO in 1996; rough scheme (a), detailed analysis of Russian contribution (b)*

Seasonal variations of contributions of main source groups to deposition to Nenets AO in absolute (a) and relative (b) values in 1996 are displayed in Figure 7.25.

Again, main contributions to depositions to the region are made by Western Europe and Russia. Here the situation is quite similar to that in Murmansk Oblast though the influence of winds of the Northern direction in the third quarter is much higher (in spite of high emission values we obtain decrease of contribution from Russian sources to depositions to Nenets AO). Further, the contributions from Russian sources to this region are twice larger than for Murmansk Oblast. As a result, relative influence of American, Chinese and Indian sources is less and we obtain slight increase of relative input of Russian sources to depositions in the fourth quarter.

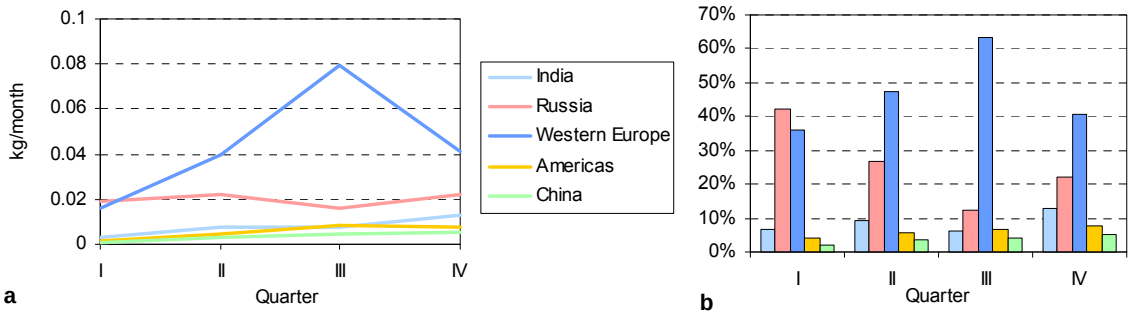

Figure 7.25. *Seasonal variations of contributions of different groups of emission sources to depositions to Nenets AO in 1996*

Yamalo-Nenets Autonomous Okrug and Taimyr Autonomous Okrug. For this region main contributors to depositions are similar to that for Nenets AO. The structure of Russian contribution to depositions here are also similar to that for Nenets AO, the influence of Ural region being further increased. The relative input from sources of Central-Chernozem, Volga, and North-Caucasian regions became even slightly larger than that from Central and Volga-Viatsky regions.

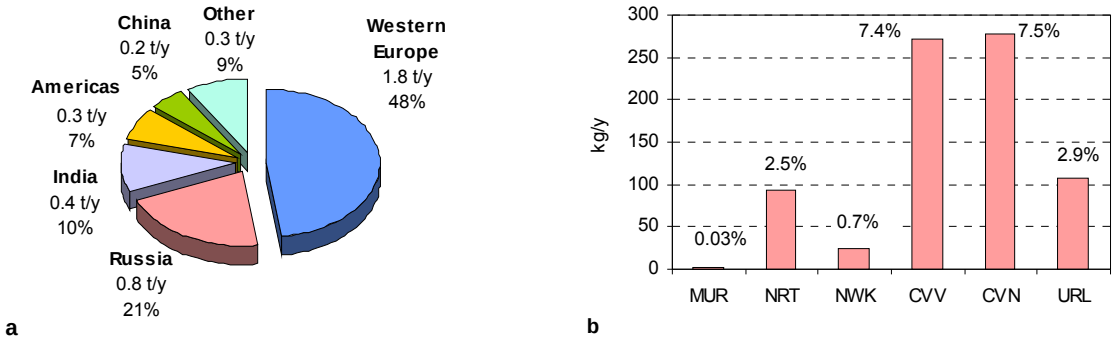

Figure 7.26. *Contributions of different emission source groups to annual depositions to Yamalo-Nenets AO and Taimyr AO in 1996; rough scheme (a), detailed analysis of Russian contribution (b)*

Seasonal variations of contributions of main source groups to deposition to Yamalo-Nenets AO and Taimyr AO in absolute (a) and relative (b) values in 1996 are shown in Figure 7.27.

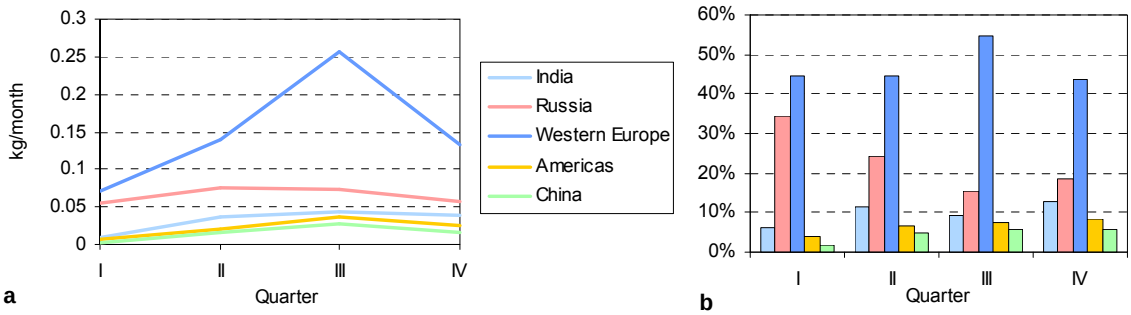

Figure 7.27. *Seasonal variations of contributions of different groups of emission sources to depositions to Yamalo-Nenets AO and Taimyr AO in 1996*

Here the situation is just the same as in Nenets AO except for the fact that the contributions from Western Europe sources are essentially decreased (up to three times) and contributions from Russian sources are increased more than twice. This leads to total increase of fraction of Russian sources in deposition to the region though temporal pattern of seasonal variation is the same as for Nenets AO.

Sakha Republic (Yakutia). Here the influence of West Europe remains to be essential with respect to depositions (36%). However, the contribution of India becomes essential (about 19%). Contributions of China, America and Russia are about the same (approximately 10%). Among Russian source groups the influence of Ural region (2%) and Central-Chernozem, Volga, and North-Caucasian regions (4.5%) increases on the account of decreasing contributions from Northern region and Central and Volga-Viatsky regions (0.8 and 3.4%, respectively).

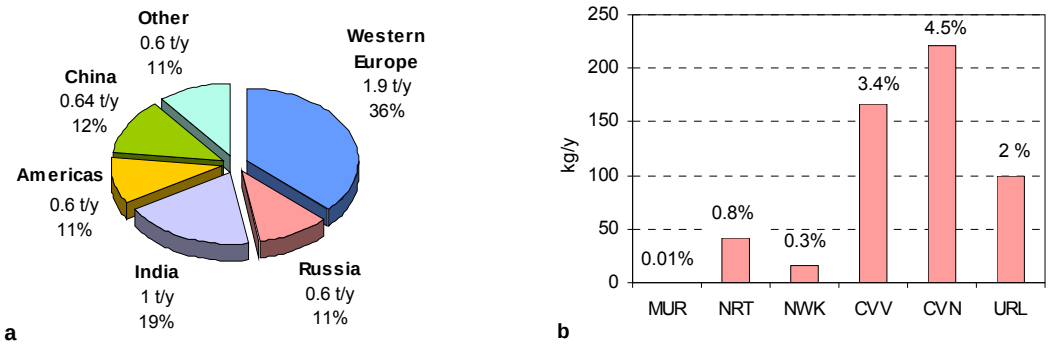

Figure 7.28. *Contributions of different emission source groups to annual depositions for Sakha Republic in 1996; rough scheme (a), detailed analysis of Russian contribution (b)*

Seasonal variations of contributions of main source groups to deposition to Sakha Republic in absolute (a) and relative (b) values in 1996 are displayed in Figure 7.29.

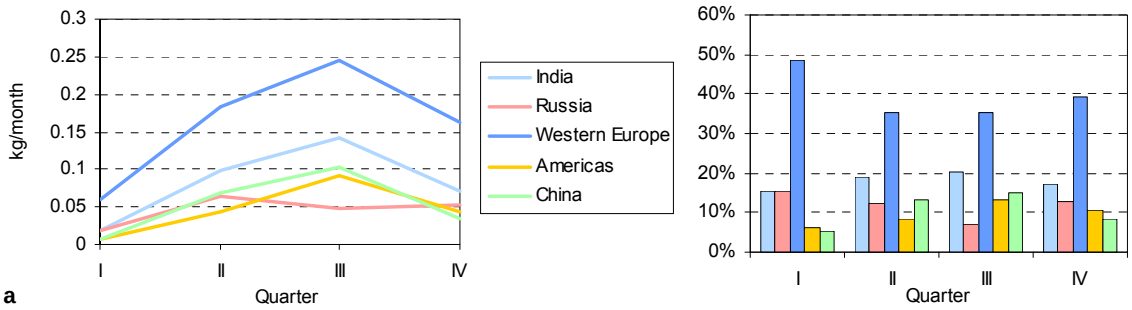

Figure 7.29. *Seasonal variations of contributions of different groups of emission sources to depositions to Sakha Republic in 1996*

The main difference of seasonal variations in this region is that contributions from American, Chinese and Indian sources in this region became more valuable than from Russian sources in second and third quarters. Due to meteorological conditions contributions of these sources are growing from first to third quarters and drop down in the fourth quarter. We recall that for Indian and Chinese sources no seasonal variations are supposed so that the mentioned seasonal variations of these sources are completely due to meteorology (the analysis of γ-HCH pathways from Indian and West-European sources is given in Section 7.1 above). Fast increase of contributions from American, Chinese and Indian sources leads to the increase of their relative input and at the same time to decrease of relative input of the contributions from West-European and Russian sources in this region in second and third quarters.

Chukotka Autonomous Okrug. For this region India becomes the main contributor to depositions together with West Europe (about 27% each). Then comes China (19%), America (11%) and Russia (5%). Contributions of all the rest sources is about 10% (Fig. 7.30).

The input of Ural region to contributions from Russian sources remains at the same level as for Sakha Republic and the inputs from Central-Chernozem, Volga, and North-Caucasian regions increased up to 2.3%.

Relative inputs from each source group to each region-receptor are explained by their geographical locations and directions of γ–HCH transport pathways over the Northern Hemisphere.

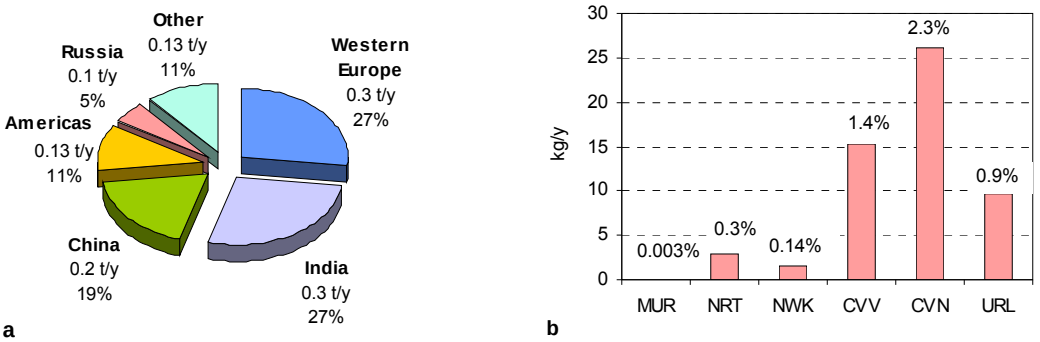

Figure 7.30. *Contributions of different emission source groups to annual depositions for Chukotka AO in 1996; rough scheme (a), detailed analysis of Russian contribution (b)*

Seasonal variations of contributions of main source groups to deposition to Chukotka AO in absolute (a) and relative (b) values in 1996 are displayed in Figure 7.31.

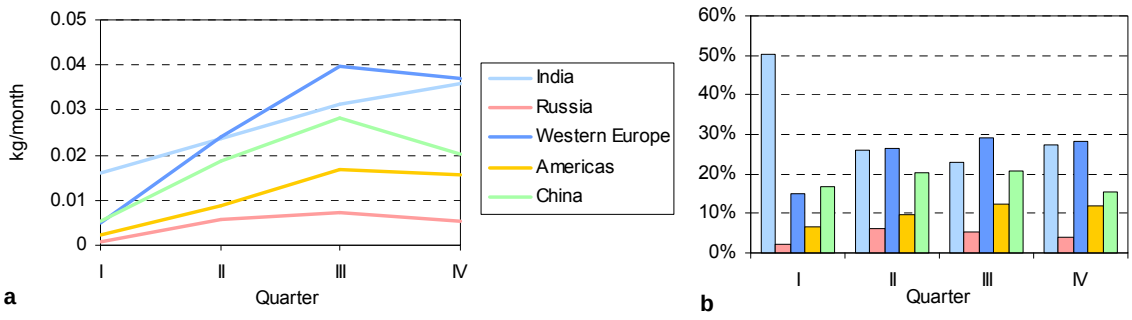

Figure 7.31. *Seasonal variations of contributions of different groups of emission sources to depositions to Chukotka AO in 1996*

Further increase of contributions from American, Chinese and Indian sources together with strong decrease of contributions from West-European and Russian sources determine the character of seasonal variations of relative inputs of different source groups in the region. These inputs from Indian sources are greater in first and fourth quarters. Inversely, for all other source groups (Russia, America, China and Western Europe) relative inputs are maximum in second and third quarters.

7.5. Concluding remarks

γ-HCH contamination levels in the Russian North, source allocation budget and pathways of γ–HCH transport were evaluated with the use of the hemispheric POP multicompartment transport model. As a result:

1. Air concentration levels in the region-receptors are within a range 0.01 – 0.09 ng/m^3, and deposition flux is from 1 to 14 g/km^2/y. Calculated air concentration levels in four regions (Murmansk Oblast, Nenets AO, Yamalo-Nenets AO and Taimyr AO, and the Sakha Republic) are close to one another. Average concentrations in Chukotka AO are two times lower. Annual averages of deposition flux values change more significantly from region to region. They decrease in the east direction. The main direction of γ–HCH marine transport is from the North-Atlantic region.

2. The main medium accumulating γ–HCH is seawater. About 80% of all γ–HCH content in the environment over the Northern Hemisphere is contained in this medium. The total calculated amount of γ-HCH deposited in the Arctic region in 1996 is equal to 78 tonnes including 58 tonnes deposited into the Arctic Ocean.

3. Contamination levels in region-receptors undergo substantial seasonal variations. These variations are due to atmospheric circulation, temperature and precipitation regime and variations in emissions.

4. The main emission sources influencing the contamination of the Russian North are West Europe, Russia, India, America and China. For the three west region-receptors (Murmansk Oblast, Nenets AO, and Yamalo-Nenets AO and Taimyr AO), the relative contributions of West-European and Russian sources are the most significant (about 50% and 20%, respectively). For eastern region-receptors (Sakha Republic and Chukotka AO), the influence of West-European sources is about 30 – 35%. Here, the relative contributions of Indian and Chinese sources are more significant (20 – 25% and 15 – 20%, respectively), influence of Russian sources becomes smaller (5 – 10%) however the influence of North American sources becomes more substantial (about 11%).

5. Contributions of different groups of Russian sources to depositions on region-receptors were evaluated. The sources from the northern region (NRT) significantly contribute to the Murmansk Oblast and Nenets AO (3%). The contribution of these sources is somewhat less to Yamalo-Nenets AO and Taimyr AO (2.5%) and relatively small to the Sakha Republic and Chukotka AO (0.8 and 0.3%, respectively). The influence of the north-western region and Kaliningrad Oblast (NWK) is relatively small on all region-receptors (from 0.1 to 1.4%). Sources from the Central and Volga-Viatsky regions affect significantly (and almost equally) all region-receptors (1.4 – 8.5%). The same is observed for sources from Central-Chernozem, Volga, and North-Caucasus regions (CVN). The contributions of Ural sources are smaller to the Murmansk Oblast (0.8%) and higher to the Sakha Republic (2%).

6. Pathways of γ–HCH transport from main source groups to region-receptors were examined. It was found that the marine pathway is significant for sea concentrations near the Russian North borders.

7. Calculations overestimate air concentrations. On the average they agree with available measurements within a factor of 2.5, with correlation 0.5. Over 50% of comparisons are within a factor of 3 and only three of them are outside of factor 5. Concentrations in precipitation agree with measurements within a factor of 1.15 on the average, with correlation 0.82. For further refinement of these estimates, refinement in emission data is needed.

References

AMAP [1998] *AMAP Assessment report: Arctic pollution issues*. Arctic Monitoring and Assessment Programme (AMAP), Oslo, Norway.

AMAP [1999], *AMAP Datareport: Atmospheric Subprogramme*, Berg T. and Hjellbrekke, NILU: OR-16-99, Norwegian Institute for Air Research, p.100.

Berg T. and A.-G.Hjellbrekke [1999] Heavy metals and POPs within the ECE region, 1997, EMEP/CCC-Report 7/99, p.98.

Berg T., A.-G.Hjellbrekke and J.E.Skjelmoen [1996] Heavy metals and POPs within the ECE region. EMEP/CCC-Report 8/96, p.187.

Berg T., A.-G.Hjellbrekke and N.Ritter [1997]. Heavy metals and POPs within the ECE region. Additional data. EMEP/CCC-Report 9/97, 79 p.

Berg T., and A.-G.Hjellbrekke [1998]. Heavy metals and POPs within the ECE region. Supplementary data for 1989-1996. EMEP/CCC-Report 7/98, p.105.

Brorström-Lundén E., E.Junedal, H.Wingfors and S.Juntto [2000] Measurements of the Atmospheric Concentrations and the Deposition Fluxes of Persistent Organic pollutants (POPs) at the Swedish West Coast and in the northern Fennoscandia, p.65.

Hallsall C.J., R.Bailey, Stern G.A., Barrie L.A., Fellin P., Muir D.C.G., Rosenberg B., Rovinsky F.Ya., Kononov E.Ya., Pastukhov B., 1998, Multi-year observations of organohalogen pesticides in the Arctic atmosphere, Environmental Pollution, v. 102, pp. 51-62.

Harner T., Kylin H., Bidleman T.F., Strachan W.M.J. [1999] Removal of α – and γ – Hexachlorocyclohexane and Enantiomers of α – Hexachlorocyclohexane in the Eastern Arctic Ocean, *Environ. Sci. Technol.,* v. 33, No. 8, pp.1157 – 1164.

Hoff R.M., W.M.J.Strachan, Sweet C.W., Chan C.H., Shackleton M., Bidleman T.F., Brice K.A., Butniston D.A., Cussion S., Gatz D.F., Harlin K., Schroeder W.H. [1996] Atmospheric deposition of toxic chemicals to the Great Lakes: a review of data through 1994. *Atmos. Environ*., v. 30, No.20, pp.3505-3527.

IADN Results to 1996, Atmospheric Deposition of Toxic Substances to the Great Lakes: IADN Results to 1996, published by Environment Canada and the United States Environmental Protection Agency, 2000, p.121.

Lövblad G., A.-G.Hjellbrekke, K.Sjoberg, J.E.Skjelmoen, J.Schaug [1995] Data Report 1993. EMEP/CCC-Report 8/95.

Pacyna J.M. et al. [1999] Final report for Project POPCYCLING-Baltic. EU DGXII, Environment and Climate Program ENV4-CT96-0214. Available on CD-rom including technical report, the emission and environmental databases as well as the POPCYCLING-Baltic model. NILU, P.O. Box 100, N-2027 Kjeller, Norway.

Review of the environmental background state over Russia in 1993. [1994] Moscow, Hydrometeoizdat, (*in Russian*).

Review of the environmental background state over Russia in 1994. [1995] Moscow, Hydrometeoizdat, (*in Russian*).

Review of the environmental background state over Russia in 1994. [1996] Moscow, Hydrometeoizdat, (*in Russian*).

Strand A. and Ø.Hov [1996] A model strategy for the simulation of chlorinated hydrocarbon distributions in the global environment. *Water, Air and Soil Pollution* v.86, pp.283-316.